Integrated Control of Bridge Type Inductive Power Transfer Systems for Light Load Efficiency Improvement

Sangjoon Ann, Jongeun Byun, Dongmyoung Joo, and Byoung Kuk Lee†

Department of Electrical and Computer Engineering
Sungkyunkwan University
Suwon, South Korea
bkleeskku@skku.edu

***Abstract*—In this paper an integrated control strategy for bridge type inductive power transfer (IPT) systems is proposed to improve light load efficiency. The proposed control method is composed of three modes: full-bridge mode, phase-shift mode, and half-bridge mode. Processes to classify the operation modes are analyzed in accordance with a wide range of coupling coefficient and output power. Laboratory experiments are performed with the proposed control, and it is verified that the efficiency at 400W is improved by up to 18.6%.**

Keywords—half-bridge control; inductive power transfer; light load efficiency improvement; wireless power transfer;

I. INTRODUCTION

In an inductive power transfer (IPT) system for electric vehicles (EVs), coupling coefficient k is a significant design consideration because the k varies with parking positions and types of EVs [1]–[5]. Therefore, previous researches deal with design procedures of the IPT systems considering a wide variation of the k [4]–[7]. In accordance with the design process of [6], LCCL-S resonant network is adopted and a required secondary voltage, which is induced by primary coil current I_p, is designed at the minimum coupling coefficient k_{min}. On account of characteristics of the LCCL-S network, the I_p is constant irrespective of the k and the load at resonant frequency. If the load-independent I_p is decreased through a control or design strategy, it is possible to improve the light load efficiency because load-independent losses generally have a larger proportion of total losses at the light load condition. Since the I_p is designed at the k_{min}, the I_p can be an excessive value at the high k condition. In other words, the I_p can be decreased at the high k condition because the smaller I_p is sufficient to induce the required secondary voltage. For that reason, in the conventional IPT system, phase-shift (PS) control is applied at the high k condition in order to limit the induced secondary voltage. The previous researches deal with only the limitation of the secondary voltage, but the effect of the load-independent current I_p and the light load efficiency are not considered [6], [7]. Besides, since the PS control does not decrease the I_p remarkably, 50% duty half-bridge (HB) control can be a solution to decrease the I_p, because input voltage of the resonant network is decreased in half compared to 50% duty full-bridge (FB) control [8], [9].

In this paper, an additional HB control to decrease the I_p at the high k condition is proposed in order to improve the light load efficiency without changing the hardware of the system. Under the proposed control, the system operates in three modes according to the k and the output power. As described in [6] and [7], the basic operation modes are 50% duty FB or the PS mode. The HB mode is additionally applied when the k and the load conditions are both satisfied. First, in order to determine the k boundary conditions of the three modes, the available operation modes are analyzed by evaluating output voltage of the resonant network according to the k. Second, loss analysis of the three modes is implemented in order to determine the load boundary conditions. Based on the derived k and the load boundary conditions, a control algorithm is proposed. The proposed control is applied to 3.3kW laboratory prototype of the IPT system for EVs and the validity is experimentally verified.

II. THE PROPOSED CONTROL STRATEGY FOR BRIDGE TYPE IPT SYSTEM

A. Configuration and Specifications of the IPT System

Fig. 1 represents the 3.3kW IPT system with LCCL-S resonant network and Table I shows specifications of the system. As shown in Fig. 1, the IPT converter consists of primary side full-bridge inverter, resonant network, power pads, and secondary side diode rectifier. Based on the previous researches, the wide range of the coupling coefficient, output power, and voltage of the battery for EVs are considered. Characteristics

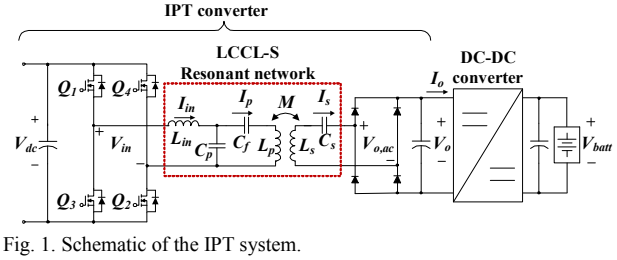

Fig. 1. Schematic of the IPT system.

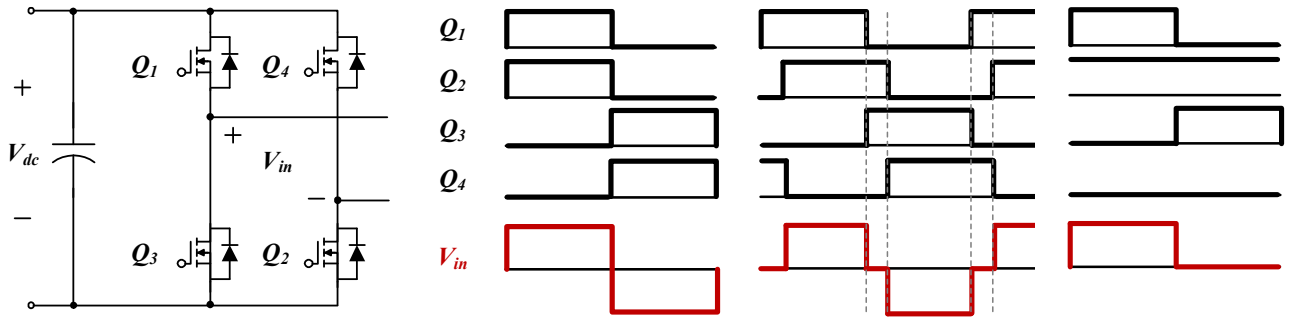

(a) Schematic (b) 50% duty FB mode (c) PS mode (d) 50% duty HB mode

Fig. 2. Operation modes of the FB inverter.

TABLE I. SPECIFICATIONS OF IPT SYSTEM

Parameter	Value [unit]
DC link voltage, V_{dc}	380 [V]
Output voltage, V_o	165-450 [V]
Output power, P_o	400-3300 [W]
Battery voltage, V_{batt}	240-410 [V]
Coupling coefficient, k	0.062-0.214

and design procedures of the system are described in [6], [7], and [10] in detail.

B. Strategies of the Proposed Control

In this paper, based on [6] and [7], basic operation modes are adopted as the FB and PS control, and an additional HB control is proposed in order to improve the light load efficiency. In other words, the HB mode is added at the specific k and load conditions. Fig. 2 shows a schematic of the FB inverter, switching signals, and input voltages of the resonant network depending on the three operation modes. Figs. 2(b) and (c) describe the 50 % duty FB and PS modes. Under the PS mode, small degrees of the input voltage of the resonant network V_{in} is cancelled by shifting phase of the gate signals in order to limit the output voltage [11]. The switching signals for the 50% duty HB control mode are described in Fig. 2(d). Under the HB mode, Q_2 keeps on and Q_4 keeps off while Q_1 and Q_3 are switching alternatively, and V_{in} is decreased in half compared to the FB mode [8], [9]. As shown in (1), AC equivalent output voltage of the LCCL-S topology can be decreased in half by applying the HB control [10], [12].

$$V_{o,ac} = \frac{2\sqrt{2}}{\pi} V_o = \frac{kV_{in}}{L_{in}\sqrt{L_p L_s}} \tag{1}$$

Besides, it should be noted that the I_p of the LCCL-S topology is a constant value at the resonant frequency regardless of the k and the load but it is proportional to the V_{in} as shown in (2).

TABLE II. COMPARISONS OF VOLTAGES AND CURRENTS BETWEEN FB MODE AND HB MODE

50% duty FB mode	50% duty HB mode	Load dependency
V_{in}	$V_{in}/2$	Independent
V_o	$V_o/2$	Independent
I_p	$I_p/2$	Independent
I_{in}	$2I_{in}$	Dependent
I_o	$2I_o$	Dependent

$$I_p = -j\frac{V_{in}}{\omega_o L_{in}} \tag{2}$$

Because of those characteristics, the I_p and V_o are decreased in half in the HB mode.

The load-independent current I_p causes load-independent losses, and these losses have a larger proportion of the total efficiency at the light load condition compared to the heavy load condition. Therefore, the light load efficiency can be improved in the HB mode compared to the FB or PS mode as shown in Table II.

III. SELECTION OF OPERATION MODES AND ALGORITHM OF THE PROPOSED CONTROL

A. Analysis of Operation Mode Selection according to the Coupling Coefficient and Load Conditions

In order to operate with high efficiency all over the range of the k and the output power, it is essential to consider not only the k, but also the load to determine the operation modes. In this section, therefore, candidates of the operation modes are firstly analyzed by considering the output voltages in accordance with the k. After that, the final operation modes considering the output power are selected through numerical loss analysis.

Fig. 3 represents the output voltages of the IPT converter in each operation mode according to the k. It should be noted that the load condition is not considered yet in Fig. 3. From k_{min} = 0.062 to k_{HB} = 0.124, the system has to operate in the FB mode

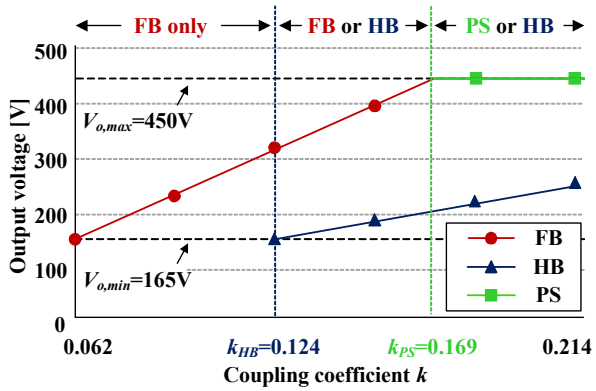

Fig. 3. Output voltages of the IPT converter in each operation mode according to the k.

only irrespective of the output power, because if the system operates in the HB mode at this k condition, the V_o could be smaller than the minimum output voltage $V_{o,min}$. From k_{HB} to k_{PS} = 0.169, the FB or HB mode can be selectively applied according to the load condition. Similarly, from k_{PS} to k_{max} = 0.214, the PS or HB mode can be selectively applied according to the load condition.

In order to determine the final operation modes, the numerical loss analysis is implemented from k_{HB} to k_{max} at 0.03 interval of the k, for determination of the load boundary condition at each k condition $P_{HB,k}$, except ferrite core and aluminum shield losses [13]–[19]. Derived efficiencies of the IPT converter from k_{HB} to k_{max} are represented in Fig. 4. As

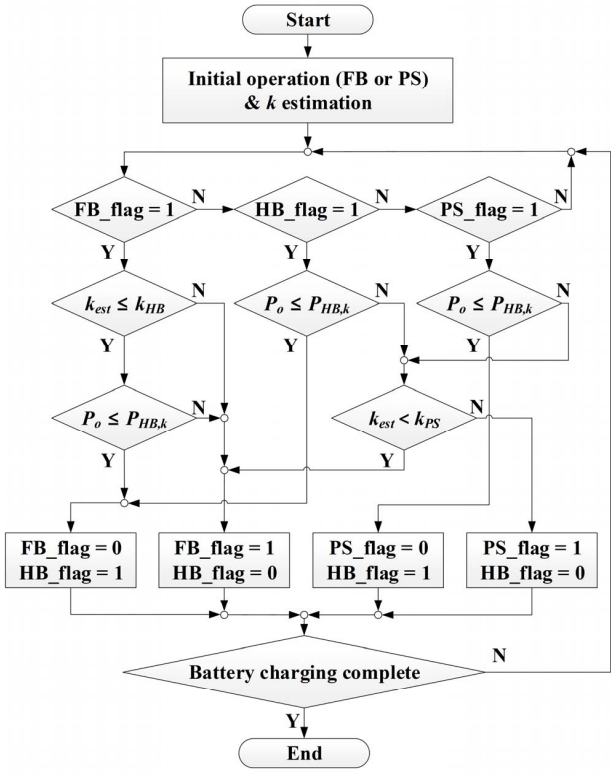

Fig. 5. Flow chart of the proposed control algorithm.

shown in Fig. 4, efficiencies of the HB mode are higher than the FB or PS modes at the light load condition because of the

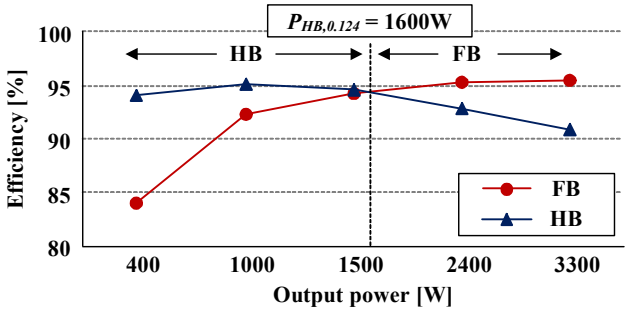

(a) k=0.124

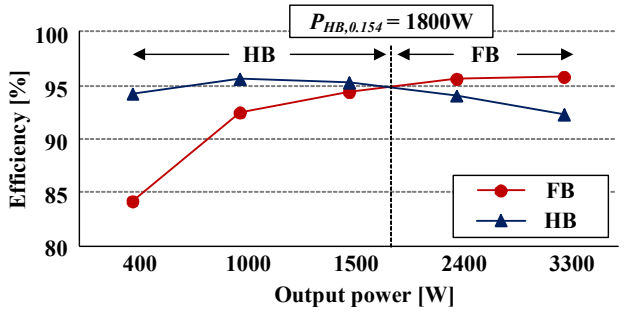

(b) k=0.154

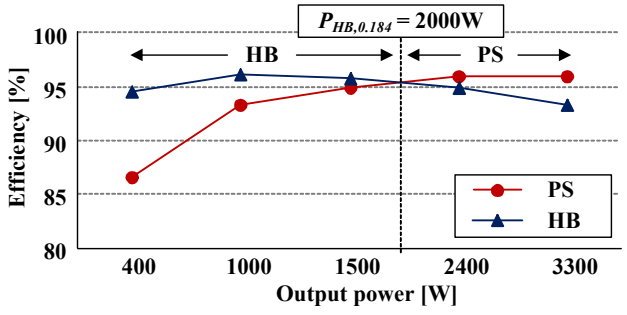

(c) k=0.184

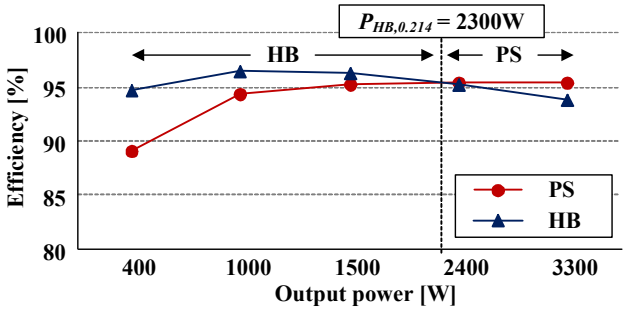

(d) k=0.214

Fig. 4. Numerical efficiency graphs according to the control methods.

decreased I_p. On the other hand, at the heavy load condition, efficiencies of the HB mode are lower than others. That is because the load-dependent input current I_{in} and the output current I_o are increased twice in the HB mode because of the decreased V_{in} and V_o, as shown in TABLE II. For those reasons, the system operates with a higher efficiency in the FB or PS mode at the heavy load condition, because dominant terms of the total losses are the load-dependent losses. Therefore, the $P_{HB,k}$ is determined as the intersecting points by comparing the efficiency graphs of the FB or PS and HB operation modes.

B. Implementation of the Proposed Control Algorithm

Fig. 5 shows a flow chart of the proposed control algorithm using the derived k_{HB}, k_{PS}, and $P_{HB,k}$. It should be noted that there are three assumptions. First, once the EVs are parked and the system starts to charge, the EVs are kept still and the k remains a constant value. Second, the system estimates the k during the initial operation. Third, the initial operation modes should be the FB or PS mode according to the estimated coupling coefficient k_{est} because the controller cannot know the initial load condition. If the HB mode is initially applied under the heavy load condition, large input and output currents can flow because of the decreased input and output voltages, and the system can get damaged. After the initial operation, the proposed control starts and the controller determines the appropriate operation mode by considering the k_{est} and the present output power P_o. If the k_{est} is less than k_{HB}, the system has to operate in the FB mode irrespective of the P_o, as described in Fig. 3. If the k_{est} is greater than or equal to k_{HB} and less than or equal to k_{max} when the P_o is less than or equal to the $P_{HB,k}$ ($k_{HB} \le k_{est} \le k_{max}$ and $P_o \le P_{HB,k}$), the system operates in the HB mode. If the P_o is greater than the $P_{HB,k}$ ($P_o > P_{HB,k}$), the system operates in the FB or PS mode. When the k is less than k_{PS} ($k < k_{PS}$), the system operates under the FB mode. On the other hand, when the k is greater than or equal to k_{PS} ($k \ge k_{PS}$), the operation mode is set to the PS mode.

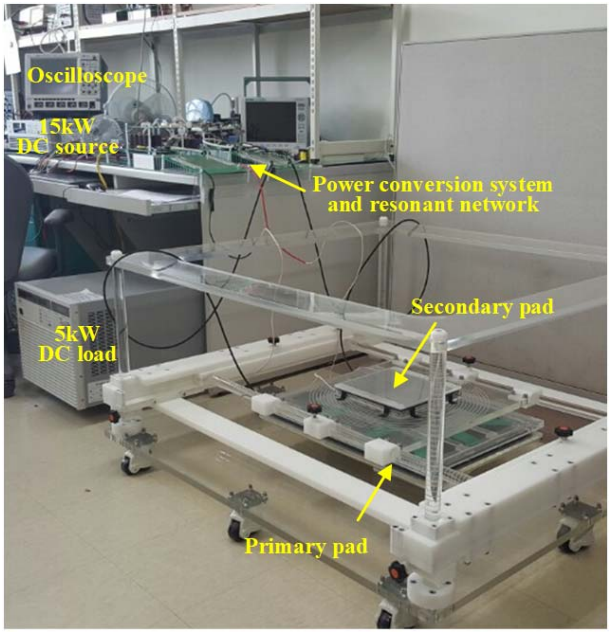

Fig. 6. 3.3kW laboratory prototype of the IPT system.

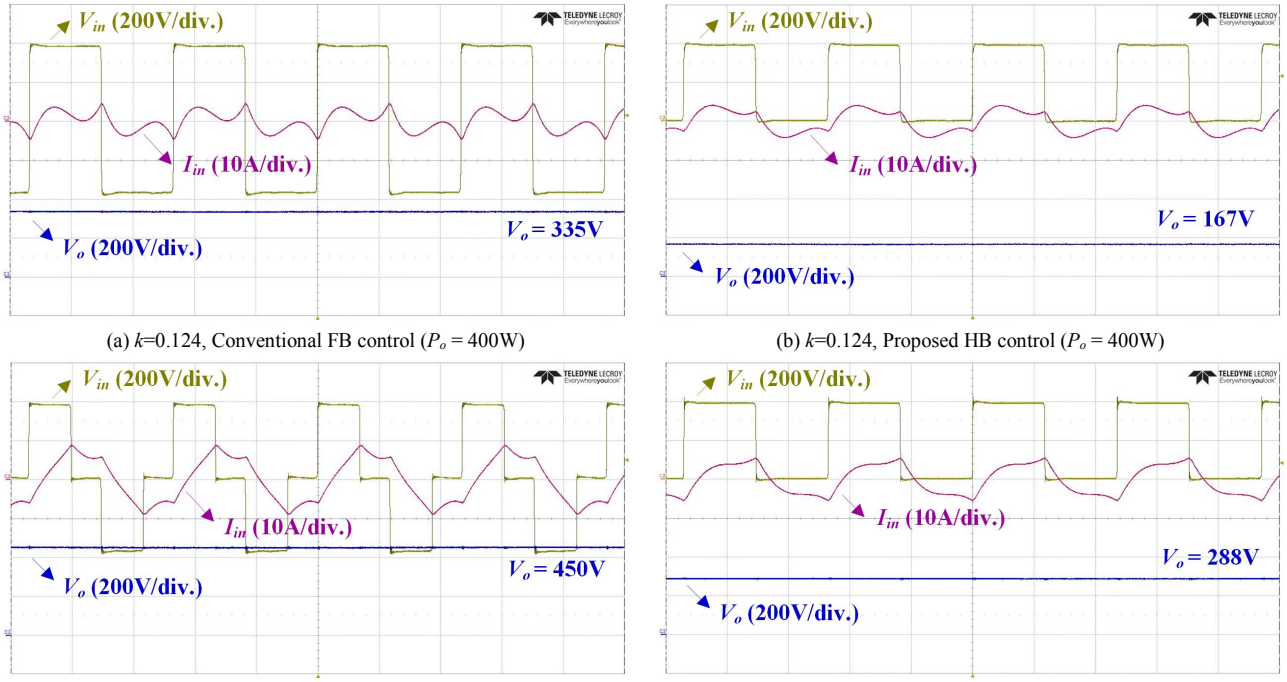

(a) k=0.124, Conventional FB control (P_o = 400W)

(b) k=0.124, Proposed HB control (P_o = 400W)

(c) k=0.214, Conventional PS control (P_o = 400W)

(d) k=0.214, Proposed HB control (P_o = 400W)

Fig. 7. Experimental waveforms in accordance with the operation modes at 400W.

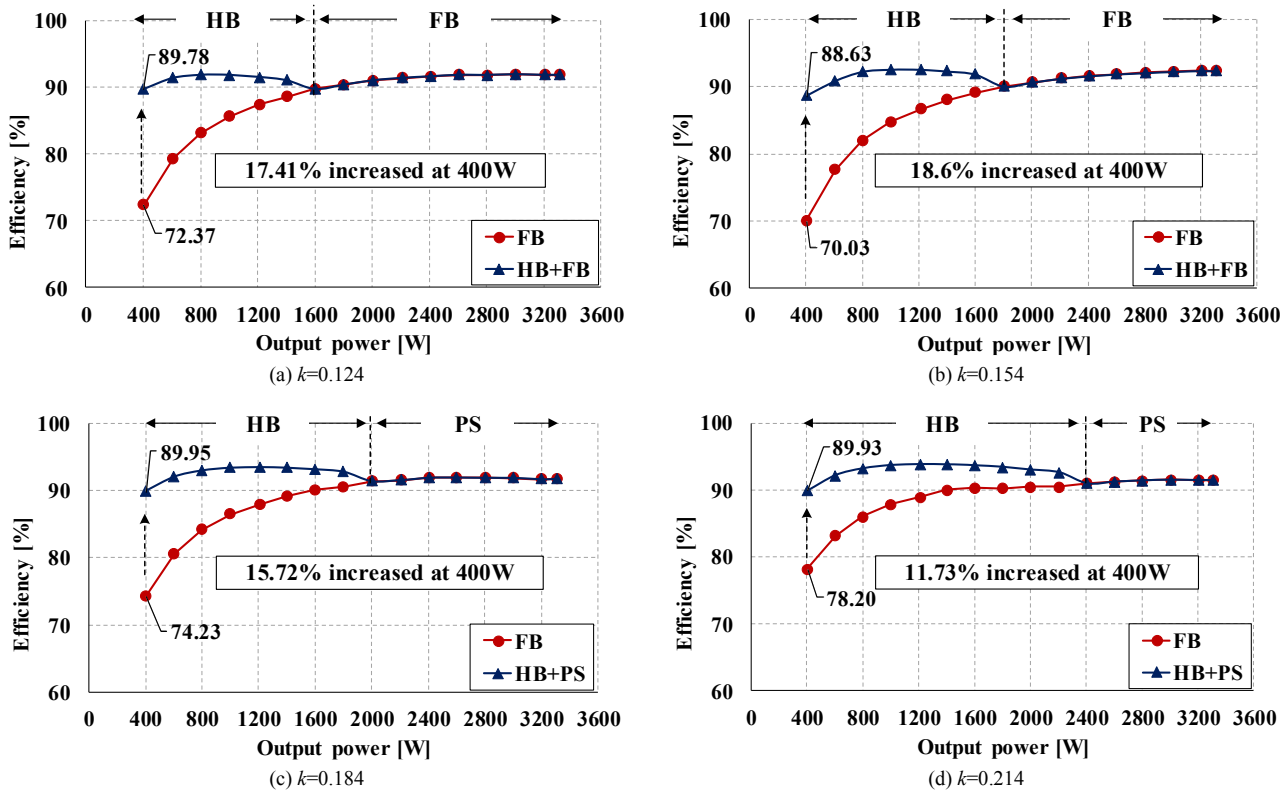

Fig. 8. Efficiencies of the prototype according to the load variation at various k conditions.

IV. Experimental Results

As shown in Fig. 6, in order to verify the proposed control strategy and the numerical analysis, a 3.3kW laboratory prototype of the IPT system for EVs is manufactured, and Fig. 7 shows the experimental waveforms of the conventional FB or PS control and the proposed HB control at light load condition (P_o = 400W) under two k conditions (k = 0.124 and k = 0.214). As shown in Fig. 7, the proposed HB control can decrease the input and output voltage of the resonant network in half. In order to compare efficiencies of the conventional control and the proposed control, efficiencies of the IPT converter are measured in accordance with the load from k_{HB} = 0.124 to k_{max} = 0.214 at 0.03 interval of the k. As shown in Fig. 8, it is verified that the proposed control can improve the efficiency of the IPT converter up to 18.6% at k = 0.154 and P_o = 400W.

V. Conclusion

In this paper, an integrated control strategy for the bridge type IPT system utilizing full-bridge, phase-shift, and half-bridge controls is proposed to improve light load efficiency. In order to apply the proposed control, boundary conditions of coupling coefficient and output power for each operation mode are classified by analyzing output voltage and numerical loss analysis considering a wide range of the coupling coefficient and the output power. Using the derived boundary conditions, algorithm of the proposed control is established. A 3.3kW IPT converter prototype is manufactured and it is experimentally verified that the light load efficiency can be improved with the proposed control by up to 18.6% at 400W.

Acknowledgment

This work was supported by "Human Resource Program in Energy Technology" of the Korea Institute of Energy Technology Evaluation and Planning (KETEP), granted financial resource from the Ministry of Trade, Industry & Energy, Republic of Korea. (*No. 20164030200980*)

References

[1] S. Li and C. Mi, "Wireless power transfer for electric vehicle applications," *IEEE J. Emerg. Sel. Topics Power Electron.*, vol. 3, no. 1, pp. 4–17, Mar. 2015.

[2] K. Aditya and S. S. Williamson, "Design considerations for loosely coupled inductive power transfer (IPT) system for electric vehicle battery charging - A comprehensive review," *in Proc. IEEE Transp. Electrification Conf. Expo.*, 2014, pp. 1–6.

[3] O. H. Stielau and G. A. Covic, "Design of loosely coupled inductive power transfer systems," *in Proc. Int. Conf. Power Syst.*, Dec. 2000, pp. 85–90.

[4] C. S. Wang, O. H. Stielau, and G. A. Covic, "Design considerations for a contactless electric vehicle battery charger," *IEEE Trans. Ind. Electron.*, vol. 52, no. 5, pp. 1308-1314, Oct. 2005.

[5] H. Takanashi, Y. Sato, Y. Kaneko, S. Abe, and T. Yasuda, "A large air gap 3 kW wireless power transfer system for electric vehicles," *in Proc. IEEE Energy Convers. Congr. Expo.*, 2012, pp. 269–274.

[6] M. Kim, D. M. Joo, D.G. Woo, and B. K. Lee, "Design and control of inductive power transfer system for electric vehicles considering wide variation of output voltage and coupling coefficient," *in Proc. IEEE Applied Power Electron. Conf. Expo.*, Mar. 2017, pp. 3648-3653.

[7] D. G. Woo, "Optimal design and control strategy of inductive power transfer charging system for electric vehicles", Ph.D dissertation, Dept. Elect. Eng., Sungkyunkwan Univ., Suwon, 2015.

[8] Z. Liang, R. Guo, G. Wang, and A. Huang, "A new wide input range high efficiency photovoltaic inverter," *in Proc. IEEE Energy Conversion Congr. Expos.*, 2010, pp. 2937–2943.

[9] M. M. Jovanovic and B. T. Irving, "On-the-fly topology-morphing control- efficiency optimization method for LLC resonant converters operating in wide input- and/or output-voltage range," *IEEE Trans. Power Electron.*, vol. 31, no. 3, pp. 2596–2608, Mar. 2016.

[10] C. Ma, S. Ge, Y. Guo, L. Sun, and C. Liu, "Investigation of a SP/S resonant compensation network based IPT system with optimized circular pads for electric vehicles," *J. Power Electronics*, vol. 16, no. 6, pp. 2359–2367, Nov. 2016.

[11] J. M. Burdío, L. A. Barragán, F. Monterde, D. Navarro, and J. Acero, "Asymmetrical voltage-cancellation control for full-bridge series resonant inverters," *IEEE Trans. Power Electron.*, vol. 19, no. 2, pp. 461–469, Mar. 2004.

[12] R. L. Steigerwald, "A comparison of half-bridge resonant converter topologies," *IEEE Trans. Power Electron.*, vol. 3, no. 2, pp. 174–182, Apr. 1988.

[13] S. Ann, D. M. Joo, M. Kim, and B.K. Lee, "High efficiency operation of the IPT converter with full and half-bridge control for electric vehicles," *Trans. Korean Inst. Power Electron.*, vol. 22, no. 5, pp. 423-430, Oct. 2017.

[14] Z. J. Shen, Y. Xiong, X. Cheng, Y. Fu, and P. Kumar, "Power MOSFET switching loss analysis: a new insight," *in Proc. IEEE 41st Ind. Appl. Soc. Annu. Meet. Conf. Rec. Ind. Appl. Conf.*, Oct. 2006, pp. 1438–1442.

[15] D. Graovac, M. Purschel, and A. Kiep, "MOSFET power losses calculation using the data-sheet parameters," Infineon Technol., Dresden, Germany, Application note, vol. 1.1, Jul. 2006.

[16] STMicroelectronics, "Calculation of conduction losses in a power rectifier," [Online]. Available: http://www.st.com/content/st_com/en.html

[17] P. Haaf, J. Harper, "Understanding diode reverse recovery and its effect on switching losses," Fairchild Semicondoctor, Europe, Tech. note.

[18] Changsung corporation, "Magnetic power cores," [Online]. Available: http://www.changsung.com/_eng/.

[19] Rubycon corporation, "Technical notes for electrolytic capacitor," [Online]. Available: http://www.st.com/content/st_com/en.html.